

# SURFACE PROPERTIES OF A NANOCRYSTALLINE Fe-Ni-Nb-B ALLOY AFTER NEUTRON IRRADIATION

*Milan Pavúk, Jozef Šitek, Katarína Sedláčková*

*Institute of Nuclear and Physical Engineering, Slovak University of Technology  
in Bratislava, Ilkovičova 3, 812 19 Bratislava, Slovak Republic*

*E-mail: milan.pavuk@stuba.sk*

*Received 15 May 2014; accepted 25 May 2014*

## 1. Introduction

For the amorphous Fe-Si-Nb-B-Cu alloy it was shown, that in certain cases radiation may have also a positive impact on the physical properties of the material. For example, the  $\text{Fe}_{73.5}\text{Si}_{13.5}\text{Nb}_3\text{B}_9\text{Cu}_1$  ribbon annealed below the crystallization temperature shall regain after irradiation with neutrons the ductility, which it had in the as-quenched state [1]. An amorphous thin film of the same composition, in turn, exhibits smaller magnetic anisotropy and coercivity after irradiation with heavy ions [2]. The positive reports mentioned above, were observed only for amorphous system. This presents a good motivation for other studies of radiation effects in nanocrystalline alloys. Once we understand that the structural changes caused by irradiation led to improvement of some physical property, design of better structures would be possible. In addition, it appears that amorphous (and possibly later nanocrystalline) alloys are already considered for applications requiring radiation resistance [3,4]. This is given by their good soft magnetic properties.

The  $(\text{Fe}_{1-x}\text{Ni}_x)_{81}\text{Nb}_7\text{B}_{12}$  alloy system becomes attractive because of the change in the crystalline structure of nanograins from bcc to fcc [5-7]. This is due to the increase in the Ni content at the expense of the Fe content. In alloys with low Ni concentration ( $x \leq 1/7$ ), only nanograins with bcc crystalline structure are formed in the first stage of crystallization. At higher Ni concentrations ( $1/4 < x \leq 1/3$ ), a structure with coexisting bcc and fcc crystalline grains is formed. The alloy with the same content of Fe and Ni ( $x = 1/2$ ) forms in the first stage of crystallization only the fcc-FeNi phase. The alloys with a substantial share of Ni ( $x > 1/2$ ) contain besides the ferromagnetic fcc-FeNi phase, also the paramagnetic fcc- $(\text{FeNi})_{23}\text{B}_6$  phase. Nanograins with an fcc lattice are not commonly seen in any class of the nanocrystalline alloys.

In this work, we studied the impact of a neutron radiation on the surface properties of the nanocrystalline  $(\text{Fe}_{0.25}\text{Ni}_{0.75})_{81}\text{Nb}_7\text{B}_{12}$  alloy. Changes in topography and domain structure were observed by means of magnetic force microscopy (MFM).

## 2. Experimental details

The amorphous  $(\text{Fe}_{0.25}\text{Ni}_{0.75})_{81}\text{Nb}_7\text{B}_{12}$  ribbon was produced by the planar flow casting process in the form of a ribbon, 10 mm wide and 25  $\mu\text{m}$  thick. About 2.5 cm long cuttings were then taken from the ribbon. These were subsequently annealed in vacuum at the temperature of 550 °C for 1 hour. By this procedure, we prepared samples of the  $(\text{Fe}_{0.25}\text{Ni}_{0.75})_{81}\text{Nb}_7\text{B}_{12}$  alloy with nanocrystalline microstructure. Two of the nanocrystalline samples were irradiated in the TRIGA Mark-II reactor in Vienna – the first one with the neutron fluence of  $1 \times 10^{16} \text{ cm}^{-2}$  and the second with the neutron fluence of  $1 \times 10^{17} \text{ cm}^{-2}$ .

The Dimension Edge™ (Veeco Instruments Inc., Santa Barbara, CA, USA) atomic force microscope (AFM) was used to study the surface properties of the samples. We focused

only on the air (shiny) side of the ribbons. Each ribbon sample was rotated under the AFM in order to achieve the scanning direction perpendicular to the longitudinal ribbon axis, which corresponds to the production direction. Thus, all AFM/MFM images presented in this paper are oriented with their vertical sides parallel to the longitudinal ribbon axis. Our probe was a Si tip with Co and Cr coating. The tip has a nominal radius of 35 nm. The maximum tip radius declared by the manufacturer (Bruker, Camarillo, CA, USA) is 50 nm. The resolution of the images is  $512 \times 512$  pixels (data points).

The first measurements of the nanocrystalline  $(\text{Fe}_{0.25}\text{Ni}_{0.75})_{81}\text{Nb}_7\text{B}_{12}$  alloy revealed that MFM signal of the irradiated specimens was basically at the detection limit of the microscope. It is important to realize that the MFM technique is sensitive only to the  $z$ -component of the stray magnetic field [8]. In order to enhance the MFM contrast, samples of the ribbon were magnetized before they were attached to an AFM sample holder. A probe magnetizer from MFM tool kit (Veeco Instruments, Santa Barbara, CA, USA) was used for this purpose. The magnetic field was oriented perpendicular to the ribbon surface. This procedure enhanced the MFM contrast significantly. Mutual orientation of the magnet and the ribbon was preserved among all samples.

### 3. Results and discussion

Fig. 1 shows the topography and Fig. 2 the domain structure of the nanocrystalline  $(\text{Fe}_{0.25}\text{Ni}_{0.75})_{81}\text{Nb}_7\text{B}_{12}$  ribbon. The images were obtained by the atomic force microscope operating in MFM mode.

The surface of non-irradiated sample (Fig. 1a) is covered by very small protrusions. Their average height is around 1 nm. The protrusions cover the entire scanned area. The equally high protrusions were also found in different locations on the surface. The first stage of structural transformation of this alloy is associated with formation of an extremely fine-grained crystalline fcc-FeNi phase [7]. Therefore, we assume that the observed protrusions are nanocrystalline grains (FeNi). It is noteworthy that the alloy with this elemental composition retains a fine-grain structure also on the surface. According to Herzer [9], the random magnetocrystalline anisotropy of such small grains is suppressed by exchange interaction and the character of the domains is determined by residual anisotropies. The non-irradiated sample had a chaotic domain structure (Fig. 2a). Comparing the size of the recorded area shown in Fig. 2a and Fig. 1a it can be seen that the domains (b/w stripes in Fig. 2a) with their sizes overlap a large number of grains.

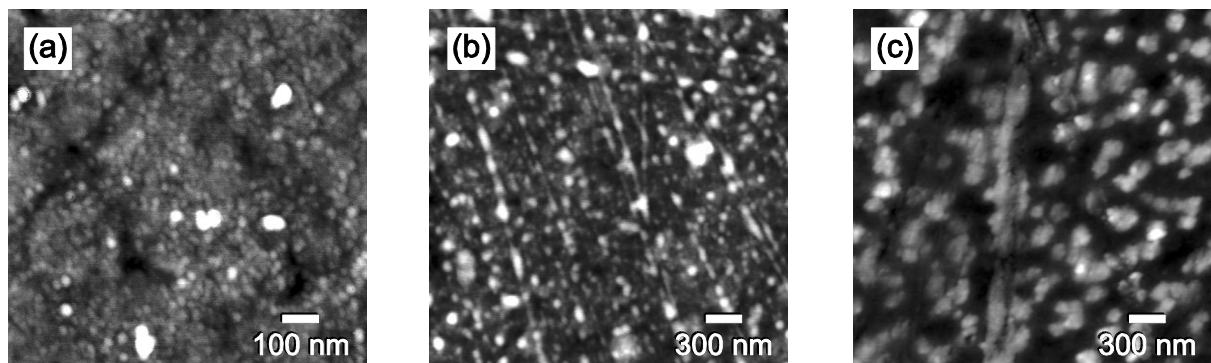


Fig. 1: Topography of the nanocrystalline  $(\text{Fe}_{0.25}\text{Ni}_{0.75})_{81}\text{Nb}_7\text{B}_{12}$  alloy: Non-irradiated sample (a), sample irradiated with the neutron fluence of  $1 \times 10^{16} \text{ cm}^{-2}$  (b), sample irradiated with the neutron fluence of  $1 \times 10^{17} \text{ cm}^{-2}$  (c). The size of the scanned area is  $1 \times 1 \mu\text{m}^2$  and  $3 \times 3 \mu\text{m}^2$  for (a) and (b, c), respectively. Note: in AFM, lateral dimensions of surface objects are affected by tip-sample convolution and therefore seem to be wider than they really are.

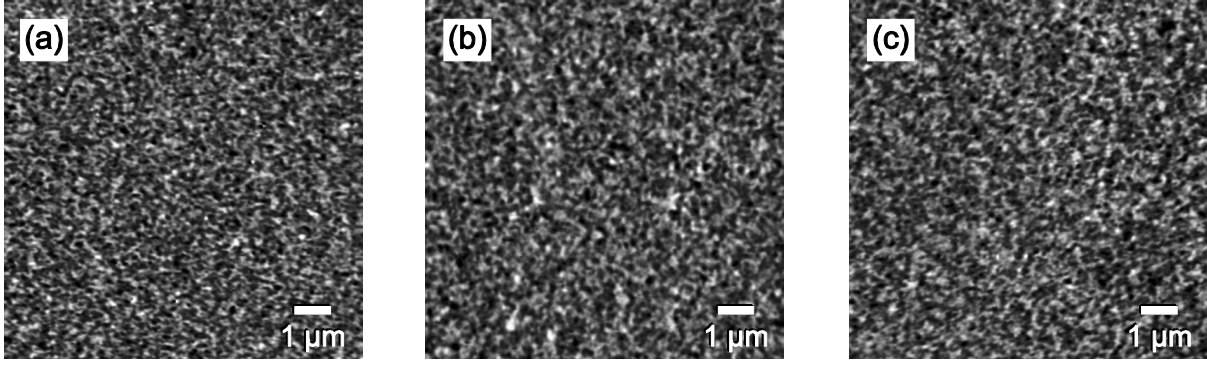


Fig. 2: Domain structure on the surface of the nanocrystalline  $(\text{Fe}_{0.25}\text{Ni}_{0.75})_{81}\text{Nb}_7\text{B}_{12}$  ribbon: Non-irradiated sample (a), sample irradiated with the neutron fluence of  $1 \times 10^{16} \text{ cm}^{-2}$  (b), sample irradiated with the neutron fluence of  $1 \times 10^{17} \text{ cm}^{-2}$  (c). The size of the scanned area is  $10 \times 10 \mu\text{m}^2$ . The images of the domain structure were recorded at a distance of 40 nm from the surface.

The topography of the sample irradiated with the neutron fluence of  $1 \times 10^{16} \text{ cm}^{-2}$  is shown in Fig. 1b. Compared to the non-irradiated sample, the average height of protrusions increased to ca. 6 nm.

The last  $(\text{Fe}_{0.25}\text{Ni}_{0.75})_{81}\text{Nb}_7\text{B}_{12}$  sample was irradiated with the highest neutron fluence of  $1 \times 10^{17} \text{ cm}^{-2}$ . In the topography, isolated protrusions are clearly visible (Fig. 1c). Their average height is about 14 nm (determined from the area of  $10 \times 10 \mu\text{m}^2$ ). After comparing numerous scans obtained from different regions of the surface we found differences in the average height of protrusions. It ranged from 12 nm to 19 nm, depending on the location. Within smaller areas ( $10 \times 10 \mu\text{m}^2$ ), the height of the individual protrusions did not change much.

From the topographic measurements of the nanocrystalline  $(\text{Fe}_{0.25}\text{Ni}_{0.75})_{81}\text{Nb}_7\text{B}_{12}$  alloy we found out that the average height of protrusions on the sample surface grew with the increasing neutron fluence. This suggests that during neutron irradiation, the temperature on the sample surface increased, and consequently the growth of already existing crystals was supported. Nevertheless, on the samples irradiated with the neutron fluences of  $1 \times 10^{16} \text{ cm}^{-2}$  (Fig. 2a) and  $1 \times 10^{17} \text{ cm}^{-2}$  (Fig. 2b) we have not observed any qualitative change in their surface domain structure. Using power spectral density (PSD) analysis, we found that the domain structures in Fig. 2 do not have any preferential arrangement of domains.

#### 4. Conclusions

By means of MFM, we studied the topography and domain structure of the as-prepared and neutron-irradiated nanocrystalline  $(\text{Fe}_{0.25}\text{Ni}_{0.75})_{81}\text{Nb}_7\text{B}_{12}$  alloy. No significant changes found in domain structure of the irradiated samples of the nanocrystalline  $(\text{Fe}_{0.25}\text{Ni}_{0.75})_{81}\text{Nb}_7\text{B}_{12}$  alloy indicates, that the alloy is well able to withstand neutron radiation up to a fluence of  $1 \times 10^{17} \text{ cm}^{-2}$ . In terms of topography, changes in the size of protrusions were observed. The round protrusions, which may be ascribed to nanocrystalline grains, grew with the increasing radiation fluence. Even in the most irradiated sample, however, the average height of protrusions did not exceed 19 nm. Based on this, we can conclude that the sizes of the crystalline grains are still within the nanometre range (probably at the level of tens of nanometres). So, one of the necessary conditions required for the preservation of favourable magnetic properties of the investigated alloy was met.

## Acknowledgement

The master ribbon was supplied by P. Švec from Slovak Academy of Sciences in Bratislava. This work was supported by the Ministry of Education, Science, Research and Sport of the Slovak Republic via the project VEGA 1/0286/12.

## References:

- [1] I. Škorvánek, R. Gerling, T. Graf, M. Fricke, J. Hesse: *IEEE Trans. Magn.*, **30**(2), 548 (1994).
- [2] R. Dubey, A. Gupta, P. Sharma, N. Darowski, G. Schumacher: *J. Magn. Magn. Mater.*, **310**, 2491 (2007).
- [3] P. Spiller, K. Blasche, B. Franczak, M. Kirk, P. Hülsmann, C. Omet, S. Ratschow, J. Stadlmann: *Nucl. Instrum. Methods Phys. Res., Sect. A*, **544**, 117 (2005).
- [4] M. Miglierini, A. Lančok, M. Pavlovič: In: *ISIAME 2008*, E. Kuzmann, K. Lázár (eds.), 17-22 August 2008, Budapest, Hungary, 45 (2009).
- [5] J. Turčanová, J. Marcin, J. Kováč, D. Janičkovič, P. Švec, I. Škorvánek: *J. Phys.: Conf. Ser.*, **144**, 012065 (2009).
- [6] P. Švec, J. Turčanová, D. Janičkovič, I. Škorvánek, P. Švec Sr.: *J. Phys.: Conf. Ser.*, **144**, 012092 (2009).
- [7] P. Švec, M. Miglierini, J. Dekan, J. Turčanová, G. Vlasák, I. Škorvánek, D. Janičkovič, P. Švec Sr.: *IEEE Trans. Magn.*, **46**(2), 412 (2010).
- [8] S. Pergolini, G. Valdre: *Nanostruct. Mater.*, **9**, 627 (1997).
- [9] G. Herzer, *IEEE Trans. Magn.*, **25**, 3327 (1989).